



# Applied Mathematics and Nonlinear Sciences

<http://journals.up4sciences.org>

## Influence of velocity slip and temperature jump conditions on the peristaltic flow of a Jeffrey fluid in contact with a Newtonian fluid

K. Vajravelu<sup>1†</sup>, S. Sreenadh<sup>2</sup> and R. Saravana<sup>3</sup>.

<sup>1</sup> Department of Mathematics, University of Central Florida Department of Mechanical, Materials and Aerospace Engineering University of Central Florida Orlando, Florida 32816-1364, USA

<sup>2</sup> Department of Mathematics Sri Venkateswara University, Tirupati 517 502, INDIA

<sup>3</sup> Department of Mathematics Madanapalle Institute of Technology and Science Madanapalle 517325, INDIA

---

### Submission Info

Communicated by Juan L. G. Guirao

Received 5th April 2017

Accepted 18th October 2017

Available online 18th October 2017

---

### Abstract

In this paper, we investigate the peristaltic transport of a two layered fluid model consisting of a Jeffrey fluid in the core region and a Newtonian fluid in the peripheral region. The channel is bounded by permeable heat conducting walls. The analysis is carried out in the wave reference frame under the assumptions of long wave length and low Reynolds number. The analytical expressions for stream function, temperature field, pressure-rise and the frictional force per wavelength in both the regions are obtained. The effects of the physical parameters associated with the flow and heat transfer are presented graphically and analyzed. It is noticed that the pressure rise decrease with increasing slip parameter  $\beta$  in the pumping region ( $\Delta P > 0$ ). The temperature field decreases with increasing Jeffrey number and the velocity slip parameter; whereas the temperature field increases with increasing thermal slip parameter. Furthermore, the size of the trapped bolus increases with increasing Jeffrey number and decreases with increasing slip parameter. We believe that this model can help in understanding the behavior of two immiscible physiological fluids in living objects.

---

**Keywords:** Peristalsis, two-layer flow, trapping phenomenon, Jeffrey fluid, Newtonian fluid, heat transfer.

**AMS 2010 codes:** 76A05, 76Z05.

---

## 1 Introduction

Peristalsis is an essential mechanism of fluid transport in biological processes. Mathematical models on peristaltic transport with single fluid and their applications to the physiological fluid mechanics have been reported

---

<sup>†</sup>Corresponding author.

Email address: [kuppalapalle.vajravelu@ucf.edu](mailto:kuppalapalle.vajravelu@ucf.edu)

extensively in the literature (see Refs. [6, 13, 14, 26, 30]). The flow of physiological fluids in different organs of living body systems such as blood through micro-vessels, capillaries and veins; food through esophagus; chyme through small intestine; and the urine through ureter has a wall like structure, which perform the pumping is normally coated with a fluid of different properties from those fluids being pumped. In order to examine the influence of fluid coating on the transport, the single phase fluid analysis of peristaltic pumping has been extended to two phase fluid analysis.

At low shear rate, the rheology of human blood in micro-circulation with connecting vessels of diameter smaller than  $500 \mu\text{m}$  obeys the properties of non-Newtonian fluids. It is speculated that the rheological behavior of non-Newtonian physiological fluid exhibits the characteristics of Jeffrey model involving time derivatives [7, 9, 11, 24, 36]. Several authors used this model for the blood flow through small vessels [17, 19], food bolus through esophagus [21] and movement of chyme in small intestine [20].

The experimental investigations of Bugliarello and Sevilla [3], and Cokelet [4] reveal that the blood flow in small vessels is a two layered model in which the core layer is a region of suspension of all erythrocytes and the peripheral layer consisting of plasma. Srivastava and Srivastava [27, 28] reported the peristaltic flow of two layered fluid model in non-uniform tubes and they have interpreted this model to the ductus efferentes of reproductive tract and the blood flow in small vessels. Brasseur et al. [1] studied the influence of Newtonian peripheral layer on another Newtonian fluid of different viscosity. Brasseur [2] also modelled the mucous coating effects on the peristaltic esophageal food bolus transport with two-fluid model. Peristaltic flow of two immiscible viscous fluids in a circular tube has been addressed by Ramachandra Rao and Usha [23]. Also, Ramachandra Rao and Usha [32] extended their model to two layered Power-law fluids. Some investigators have engaged in the progress of peristaltic transport of two layered fluid models [15, 29] and [33]. Very recently, Kavitha et al. [10] presented the peristaltic pumping of a Jeffrey fluid in contact with a Newtonian fluid in an inclined channel. All these authors have been reported the effects of interface shape and pressure rise with the time averaged flux.

The energy transfer in biological living systems can be identified in metabolic heat generation, blood perfusion, skin burning, hypothermia, fever, convective heat exchange between blood and tissue. The variation of temperature strongly influences the non-Newtonian behavior of blood in various parts of the circulatory system. The results of heat transfer with peristaltic flow have many biomedical and bioengineering applications such as hemodialysis, oxygenation and hypothermia therapy. Considering multi-fluid flow situations and heat transfer, Umavathi et al. [31] studied the unsteady mixed convection flow of two immiscible viscous fluids through a channel characterized by one irregular wall and one flat wall. Farooq et al. [5] analyzed the two layered flow of third grade nano-fluids in a vertical channel with viscous dissipation effects. Very recently, Ponalagusamy and Selvi [22] addressed the combined effects of plasma layer thickness, heat transfer and magnetic field on the flow of blood through stenosed arteries.

In blood vessels, glycocalyx is a thin layer of glycoproteins and proteoglycans which covers the surface of endothelial cells. The increased endothelial cell layer permeability facilitates the accumulation of low density lipoproteins in the artery wall and accelerates atherosclerosis [12]. Investigations of peristaltic flow with porous walls provide insight into the disease involved in arteries and gastrointestinal tract. Vajravelu et al. [34] examined the influence of permeable wall on the peristaltic flow of a Casson fluid in contact with a Newtonian fluid in a circular pipe by considering the Saffman slip [25] in the absence of heat transfer. The flow of non-Newtonian fluids with slip effects and heat transfer has its wide range of applications in chemical and polymer processing. Nadeem and Akram [16] obtained the exact and numerical solutions for slip effects on the peristaltic transport of a Jeffrey fluid in an asymmetric channel under the influence of induced magnetic field. A few investigations of the effects of velocity slip and temperature jump conditions on the peristaltic flow of generalized Newtonian fluid models have been reported in [8, 18, 35].

In view of the above studies, an attempt is made in this paper to study the peristaltic transport of a two-layered fluid model consisting of a core region with a Jeffrey fluid and a peripheral layer with a Newtonian fluid. The effects of the velocity slip, temperature jump boundary conditions and the heat transfer in the channel

are assessed. The results obtained throw light on the impact of peristalsis in the circulation of blood in small blood vessels and further may be useful in understanding the transport of physiological fluids in esophagus and gastrointestinal tract. Also, it is expected that the results obtained will not only provide useful information for industrial applications but also complement the earlier works.

## 2 Mathematical formulation

The constitutive equations for an incompressible Jeffrey fluid are

$$\tau = -pI + S \tag{2.1}$$

$$S = \frac{\mu_1}{1+\lambda_1} (\dot{\gamma} + \lambda_2 \ddot{\gamma}) \tag{2.2}$$

where  $\tau$  and  $S$  represent Cauchy stress tensor and extra stress tensor respectively,  $p$  is the pressure,  $I$  is the identity tensor,  $\lambda_1$  is the ratio of relaxation to retardation times,  $\lambda_2$  is the retardation time,  $\dot{\gamma}$  is shear rate, and a dot over the quantities indicates differentiation with respect to time (for details see [17]).

We consider the peristaltic flow of incompressible and immiscible physiological fluids occupying core with a Jeffrey fluid of viscosity  $\mu_1$  and in surrounding peripheral layer with a Newtonian fluid of viscosity  $\mu_2$ . Let us consider a two dimensional channel of width  $2a$ . The channel walls are maintained at constant temperature  $T_1$  Effect of thin permeable layer (attached to the flexible walls) on the flow is investigated by taking into account the velocity slip and the temperature jump conditions. Due to symmetry and for simplicity we analyze the flow in half width of the channel as shown in Fig. 1.

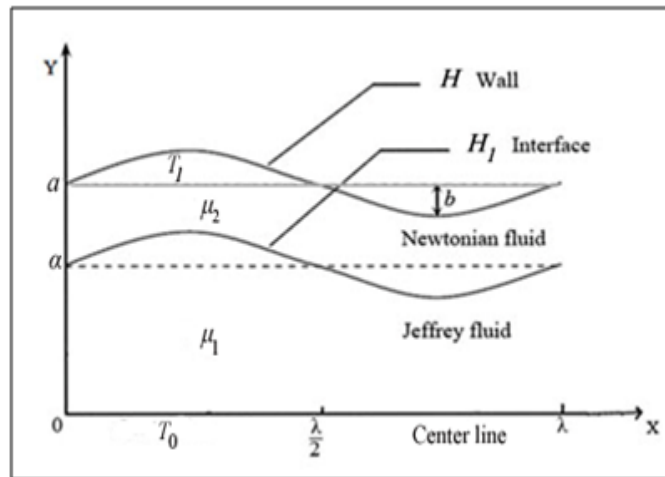


Fig. 1 Physical Model

The wall deformation due to infinite sinusoidal wave train of peristaltic wave is given by

$$Y = H(X,t) = a + b \sin \frac{2\pi}{\lambda} (X - ct) \tag{2.3}$$

where  $b$ ,  $\lambda$ ,  $c$  and  $t$  represent the amplitude, wave length, wave speed and time respectively.

The subsequent deformation of the interface separating the core and the peripheral layer is denoted by  $Y = H_1(X,t)$ , see Fig. 1 for details, which is not known a priori. The flow becomes steady in the wave frame  $(x,y)$  moving with velocity away from the laboratory frame  $(X,Y)$  in the direction of wave propagation. We

discuss the steady flow under the consideration of channel length is an integral multiple of the wavelength  $\lambda$ , the pressure difference across the ends of the channel is a constant and the periodicity of the interface is same as that of the peristaltic wave.

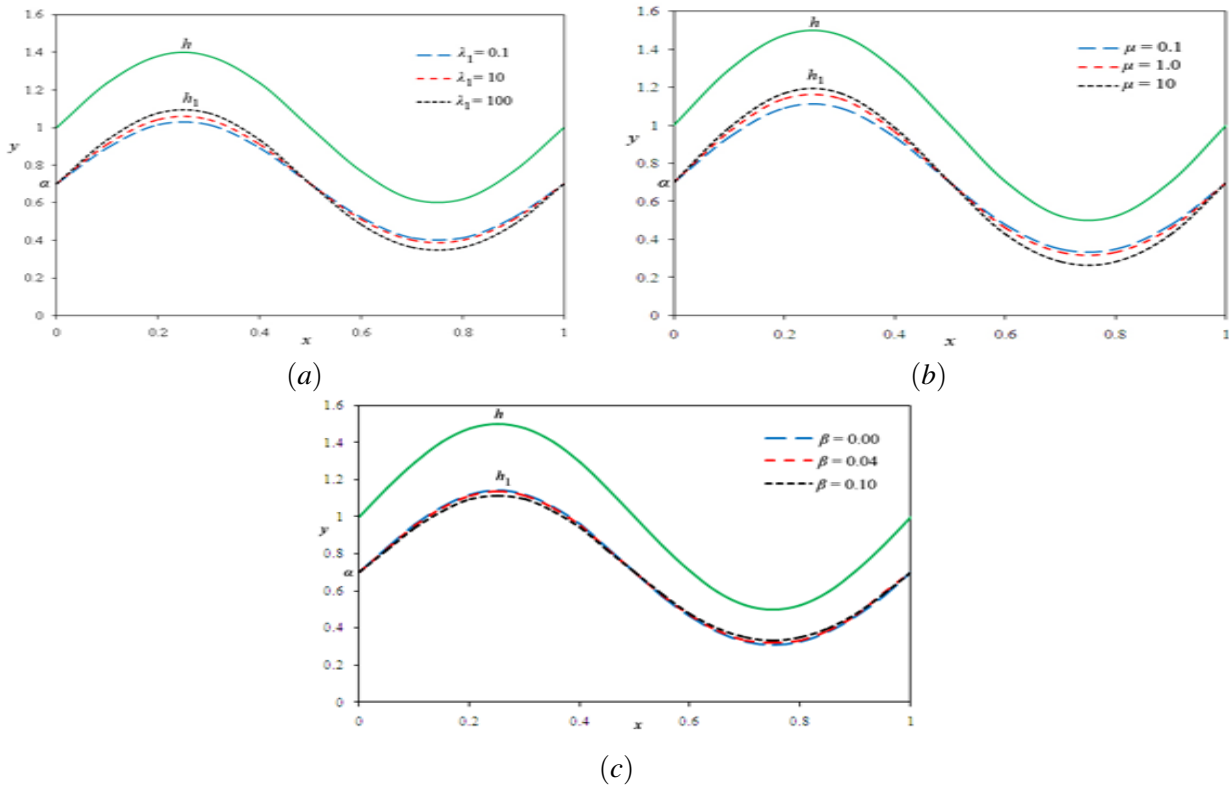


**Fig. 2** The variation of shape of interface with  $\mu = 0.1, \bar{Q} = 0.1, \alpha = 0.7$  for (a)  $\phi = 0.4, \beta = 0.1, \lambda_1 = 0.1, 10, 100$ , (b)  $\phi = 0.5, \beta = 0.1, \mu = 0.1, 1.0, 10$ , (c)  $\phi = 0.5, \mu = 0.1, \beta = 0.00, 0.04, 0.10$ .

The transformation from fixed to wave frame of references are given by

$$\left. \begin{aligned} x &= X - ct, \quad y = Y, \quad u(x, y) = U(X - ct, Y) - c, \\ v(x, y) &= V(X - ct, Y), \quad p(x) = P(X, t), \quad \psi = \Psi - Y \end{aligned} \right\} \tag{2.4}$$

where  $u, v, p$  and  $\psi$  are the velocity components, pressure and stream functions in the wave frame.  $U, V, P$  and  $\Psi$  are the velocity components, pressure and stream functions in the fixed frame respectively.

We introduce the following non-dimensional quantities;

$$\left. \begin{aligned} \bar{x} &= \frac{x}{\lambda}, \quad \bar{y} = \frac{y}{a}, \quad \bar{t} = \frac{ct}{\lambda}, \quad \bar{h} = \frac{H}{a}, \quad \bar{h}_1 = \frac{H_1}{a}, \quad \bar{p} = \frac{pa^2}{\mu_1 \lambda c}, \quad \phi = \frac{b}{a}, \quad \bar{q} = \frac{q}{ac}, \quad \bar{F} = \frac{Fa}{\mu_1 \lambda c}, \\ \bar{\psi}^{(i)} &= \frac{\psi^{(i)}}{ac}, \quad \bar{u}^{(i)} = \frac{u^{(i)}}{c} = \frac{\partial \bar{\psi}^{(i)}}{\partial \bar{y}}, \quad \bar{v}^{(i)} = \frac{v^{(i)} \lambda}{ac} = \frac{\partial \bar{\psi}^{(i)}}{\partial \bar{x}}, \quad \bar{\mu} = \begin{cases} 1, & 0 \leq \bar{y} \leq \bar{h}_1 \\ \mu, \mu \left( = \frac{\mu_2}{\mu_1} \right), & \bar{h}_1 \leq \bar{y} \leq \bar{h} \end{cases}, \\ \text{Re} &= \frac{a^2 \rho c}{\lambda \mu_1}, \quad \bar{S} = \frac{a}{\mu_1 c} S, \quad \beta = \frac{\sqrt{k_p}}{a \sigma} = \frac{\sqrt{Da}}{\sigma}, \quad \theta^{(i)} = \frac{T^{(i)} - T_0}{T_1 - T_0}, \quad v = \frac{\mu_1}{\rho}, \quad Ec = \frac{c^2}{C_p(T_1 - T_0)}, \\ \text{Pr} &= \frac{\mu_1 C_p}{k_1}, \quad \bar{k} = \begin{cases} 1, & 0 \leq \bar{y} \leq \bar{h}_1, \\ k, k \left( = \frac{k_2}{k_1} \right), & \bar{h}_1 \leq \bar{y} \leq \bar{h}. \end{cases} \end{aligned} \right\} \tag{2.5}$$

Here superscript values ( $i = 1, 2$ ) refer to the core and the peripheral flow regions respectively. The quantities

$\phi$  is the amplitude ratio,  $k_p$  is the permeability of porous material of the wall,  $\sigma$  is the dimensionless constant which depends on pore size of the permeable material,  $Da$  is the Darcy number,  $\beta$  is the slip parameter,  $T$  is the temperature,  $T_0$  is the temperature at the center line of the channel,  $C_p$  is the specific heat at a constant pressure,  $\bar{\mu}$  is the ratio of the viscosity,  $k$  is the ratio of thermal conductivities,  $Ec$  is the Eckert number, and  $Pr$  is the Prandtl number.

Under the long wave length approximation (applicable in physiological flows), the Reynolds number is small and hence the curvature and inertia terms are negligible. Thus the governing equations of two layered fluid flow reduce to (dropping bars)

$$\frac{\partial}{\partial y} \left( \frac{1}{1+\lambda_1} \frac{\partial^2 \psi^{(1)}}{\partial y^2} \right) = \frac{\partial p}{\partial x} \quad 0 \leq y \leq h_1, \tag{2.6}$$

$$\frac{\partial}{\partial y} \left( \mu \frac{\partial^2 \psi^{(2)}}{\partial y^2} \right) = \frac{\partial p}{\partial x} \quad h_1 \leq y \leq h, \tag{2.7}$$

$$0 = \frac{\partial p}{\partial y}, \tag{2.8}$$

$$\frac{\partial^2 \theta^{(1)}}{\partial y^2} + Br \left\{ \frac{1}{1+\lambda_1} \left( \frac{\partial^2 \psi^{(1)}}{\partial y^2} \right)^2 \right\} = 0 \quad 0 \leq y \leq h_1, \tag{2.9}$$

$$\frac{\partial^2 \theta^{(2)}}{\partial y^2} + k.Br \left\{ \left( \frac{\partial^2 \psi^{(2)}}{\partial y^2} \right)^2 \right\} = 0 \quad h_1 \leq y \leq h, \tag{2.10}$$

Here  $\lambda_1$  is the Jeffrey parameter and  $Br = Ec.Pr$  is the Brinkman number. The corresponding dimensionless boundary conditions are

$$\psi^{(1)} = 0 \quad \text{at} \quad y = 0, \tag{2.11}$$

$$\frac{\partial^2 \psi^{(1)}}{\partial y^2} = 0 \quad \text{at} \quad y = 0, \tag{2.12}$$

$$\psi^{(2)} = q \text{ (aconstant)} \quad \text{at} \quad y = h, \tag{2.13}$$

$$\frac{\partial \psi^{(2)}}{\partial y} + \beta \frac{\partial^2 \psi^{(2)}}{\partial y^2} = -1 \quad \text{at} \quad y = h, \tag{2.14}$$

$$\psi^{(2)} = \psi^{(1)} = q_1 \text{ (aconstant)} \quad \text{at} \quad y = h_1, \tag{2.15}$$

$$\frac{1}{1+\lambda_1} \frac{\partial^2 \psi^{(1)}}{\partial y^2} = \mu \frac{\partial^2 \psi^{(2)}}{\partial y^2} \quad \text{at} \quad y = h_1, \tag{2.16}$$

$$\frac{\partial \theta^{(1)}}{\partial y} = 0 \quad \text{at} \quad y = 0, \tag{2.17}$$

$$\theta^{(2)} + \gamma \frac{\partial \theta^{(2)}}{\partial y} = 1 \quad \text{at} \quad y = h, \tag{2.18}$$

$$\theta^{(1)} = \theta^{(2)} \quad \text{at} \quad y = h_1, \tag{2.19}$$

$$\frac{\partial \theta^{(1)}}{\partial y} = k \frac{\partial \theta^{(2)}}{\partial y} \quad \text{at} \quad y = h_1, \tag{2.20}$$

The velocity slip boundary condition Eq.(2.14) is used as in Saffman [25]. Further the velocity is continuous at the fluid interface. The temperature jump boundary condition is given in Eq.(2.18), where  $\gamma$  represents the dimensionless thermal slip parameter.

Here the total flux  $q$  is the sum of core layer flux  $q_1$  and peripheral layer flux  $q_2$  across any cross-section in the wave frame. Further the velocity and the shear stress are continuous across the interface. Due to incompressibility of the fluids and due to the lubrication theory, the fluxes  $q$ ,  $q_1$  and  $q_2$  are independent of  $x$ .

The non-dimensional average volume flow rate  $\bar{Q}$  over one wavelength  $\eta$  ( $= \frac{\lambda}{c}$ ) of the sinusoidal peristaltic wave is given by

$$\bar{Q} = q + 1 \tag{2.21}$$

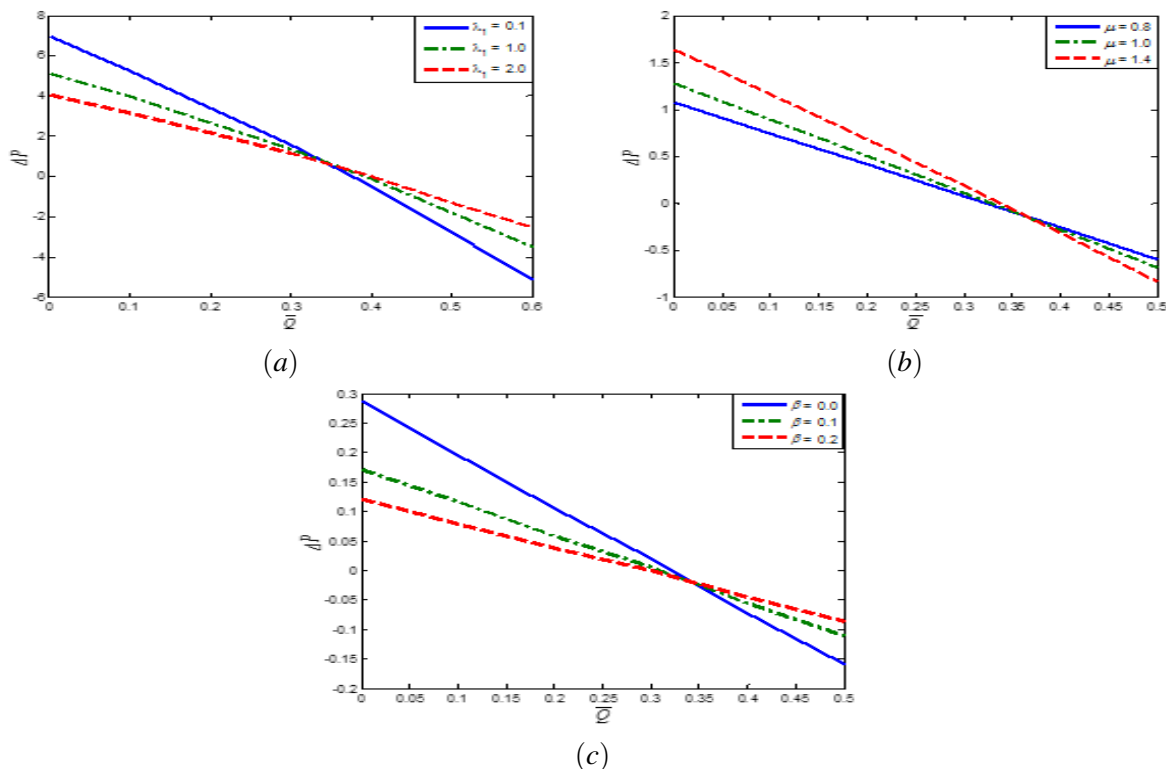


**Fig. 3** The variation of  $\Delta P$  with  $\bar{Q}$  at  $\phi = 0.5$ ,  $\alpha = 0.7$  for (a)  $\mu = 10$ ,  $\beta = 0.1$ ,  $\lambda_1 = 0.1, 1.0, 2.0$ , (b)  $\lambda_1 = 1$ ,  $\beta = 0.1$ ,  $\mu = 0.8, 1.0, 1.4$ , (c)  $\mu = 0.1$ ,  $\lambda_1 = 1$ ,  $\beta = 0.0, 0.2, 0.4$ .

### 3 Solution of the problem

Solving Eqs. (2.6)-(2.10) together with boundary conditions (2.11) -(2.20), we get

$$\psi^{(1)} = -y + \left( \frac{3(q+h)F_2 y - \mu(1+\lambda_1)(q+h)y^3}{2F_3} \right) \quad \text{for} \quad 0 \leq y \leq h_1 \tag{3.1}$$

$$\psi^{(2)} = -y + (q+h) + \left( \frac{3(q+h)h^2 y - (q+h)y^3 - (q+h)h^3 + 3\beta(q+h)h(y-h)}{2F_3} \right) \quad \text{for} \quad h_1 \leq y \leq h \tag{3.2}$$

$$\theta^{(1)} = -\frac{3Br\mu^2(1+\lambda_1)(q+h)^2}{4F_3^2} y^4 + \frac{3Br(q+h)^2(A_1+A_2)}{4kF_3^2} + 1 \quad \text{for} \quad 0 \leq y \leq h_1 \tag{3.3}$$

$$\theta^{(2)} = \frac{-3Brk(q+h)^2}{4F_3^2} y^4 + \frac{3Br(q+h)^2(k^2 - \mu^2(1+\lambda_1))h_1^3}{kF_3^2} y + \frac{3Br(q+h)^2}{4kF_3^2} A_1 + 1 \quad \text{for} \quad h_1 \leq y \leq h, \tag{3.4}$$

where

$$F_J = h^J + (\mu(1+\lambda_1) - 1)h_1^J + Jh^{J-1}\beta, \quad (J = 2, 3)$$

$$A_1 = h^3 k^2 (h + 4\gamma) - 4 (k^2 - \mu^2 (1 + \lambda_1)) (h + \gamma) h_1^3$$

$$A_2 = (3k^2 + \mu^2 (1 + \lambda_1) (k - 4)) h_1^4.$$

As  $\lambda_1 \rightarrow 0$  and  $\beta \rightarrow 0$  the results obtained in Eqs. (3.1) and (3.2) are found to be in agreement with the corresponding results of Brasseur et al. [1].

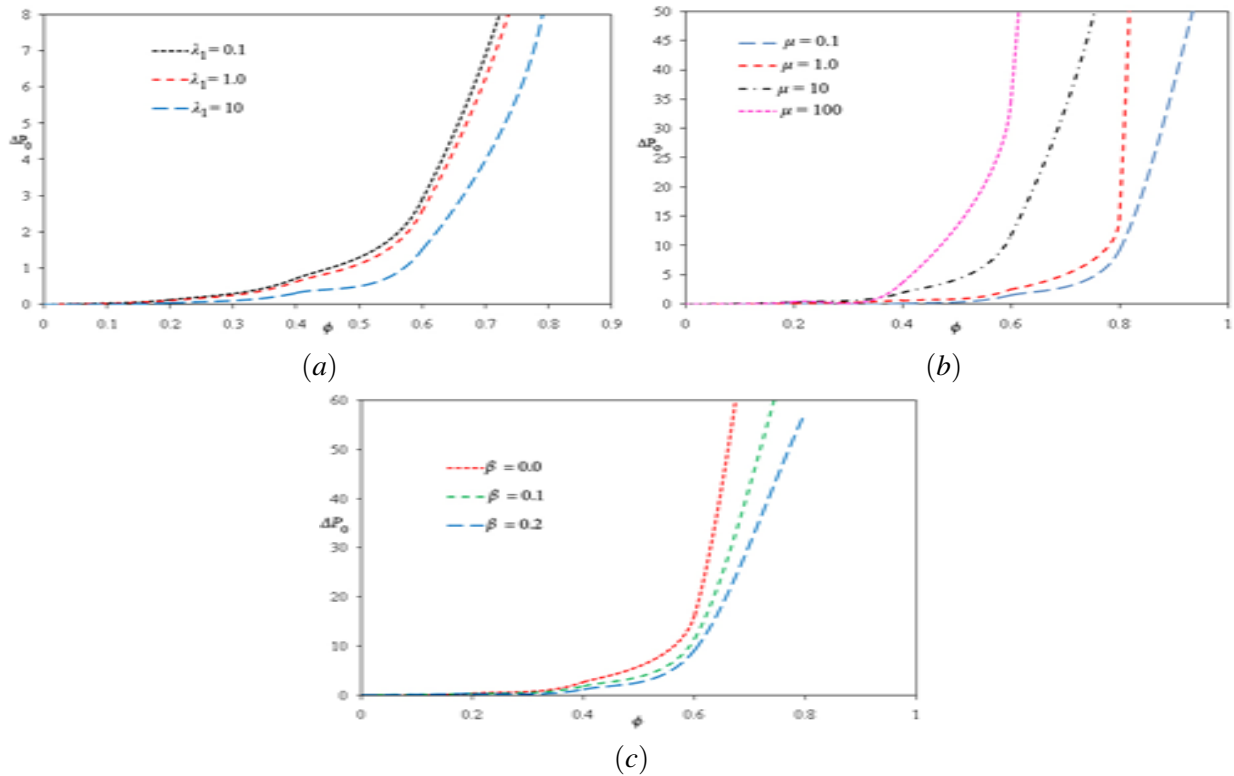


**Fig. 4** The variation of  $\Delta P_0$  with  $\phi$  at  $\alpha = 0.7$  for (a)  $\beta = 0.1, \mu = 10, \lambda_1 = 0.1, 1.0, 10$ , (b)  $\beta = 0.1, \lambda_1 = 1, \mu = 0.1, 1.0, 10, 100$ , (c)  $\lambda_1 = 1, \mu = 10, \beta = 0.0, 0.2, 0.3$ .

The axial pressure gradient is inferred from (2.6) or (2.7) as

$$\frac{dp}{dx} = -\frac{3\mu(q+h)}{F_3} \tag{3.5}$$

Integrating Eq. (3.5) over one wavelength, we get the pressure rise (drop) over one cycle of wave as

$$\Delta P = \int_0^1 \frac{dp}{dx} dx = -3\mu (\bar{Q} - 1) I_1 - 3\mu I_2 \tag{3.6}$$

where  $I_1 = \int_0^1 \frac{1}{F_3} dx$  and  $I_2 = \int_0^1 \frac{h}{F_3} dx$ .

The time average flux at zero pressure rise is denoted by  $\bar{Q}_0$  and it is given by

$$\bar{Q}_0 = 1 - \frac{I_2}{I_1} \tag{3.7}$$

and the pressure rise required to produce zero average flow rate is denoted by  $\Delta P_0$  and is given by  $\Delta P_0 = 3\mu (I_1 - I_2)$ . (3.8)

The dimensionless frictional force at the wall across one wavelength is given by

$$F = \int_0^1 h \left( -\frac{dp}{dx} \right) dx = 3\mu (\bar{Q} - 1) I_2 + 3\mu I_3 \tag{3.9}$$

where  $I_3 = \int_0^1 \frac{h^2}{F_3} dx$ .

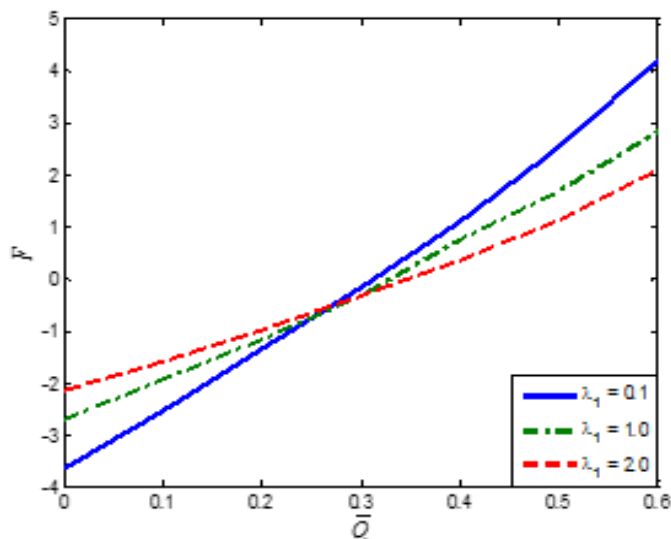


**Fig. 5** The variation of  $F$  with  $\bar{Q}$  for different values of  $\lambda_1$  with fixed  $\mu = 10, \phi = 0.5, \alpha = 0.7, \beta = 0.1$ .

#### 4 The equation for the interface

The interface is also a stream line. For a given wave geometry and the time averaged flux  $\bar{Q}$ , the unknown interface  $h_1(x)$  is determined from (3.1) and (3.2) using the boundary condition (2.15). The fourth degree algebraic equation governing the interface  $h_1(x)$  is given by

$$2(\mu(1 + \lambda_1) - 1)h_1^4 - ((q + h)(2\mu(1 + \lambda_1) - 3) - 2q_1(\mu(1 + \lambda_1) - 1))h_1^3 + (2h^3 - 3(q + h)h^2 + 6\beta h^2 - 6\beta(q + h)h)h_1 + 2q_1h^3 + 6\beta q_1h^2 = 0. \tag{4.1}$$

Since  $q$  and  $q_1$  are independent of  $x$ , we choose the condition  $h_1 = \alpha$  at  $x = 0$  in Eq. (4.1) to obtain  $q_1$  as

$$q_1 = \frac{2(1 - \mu(1 + \lambda_1))\alpha^4 + \bar{Q}(2\mu(1 + \lambda_1) - 3)\alpha^3 + (3\bar{Q} + 6\beta(\bar{Q} - 1) - 2)\alpha}{2((\mu(1 + \lambda_1) - 1)\alpha^3 + 3\beta + 1)}. \tag{4.2}$$

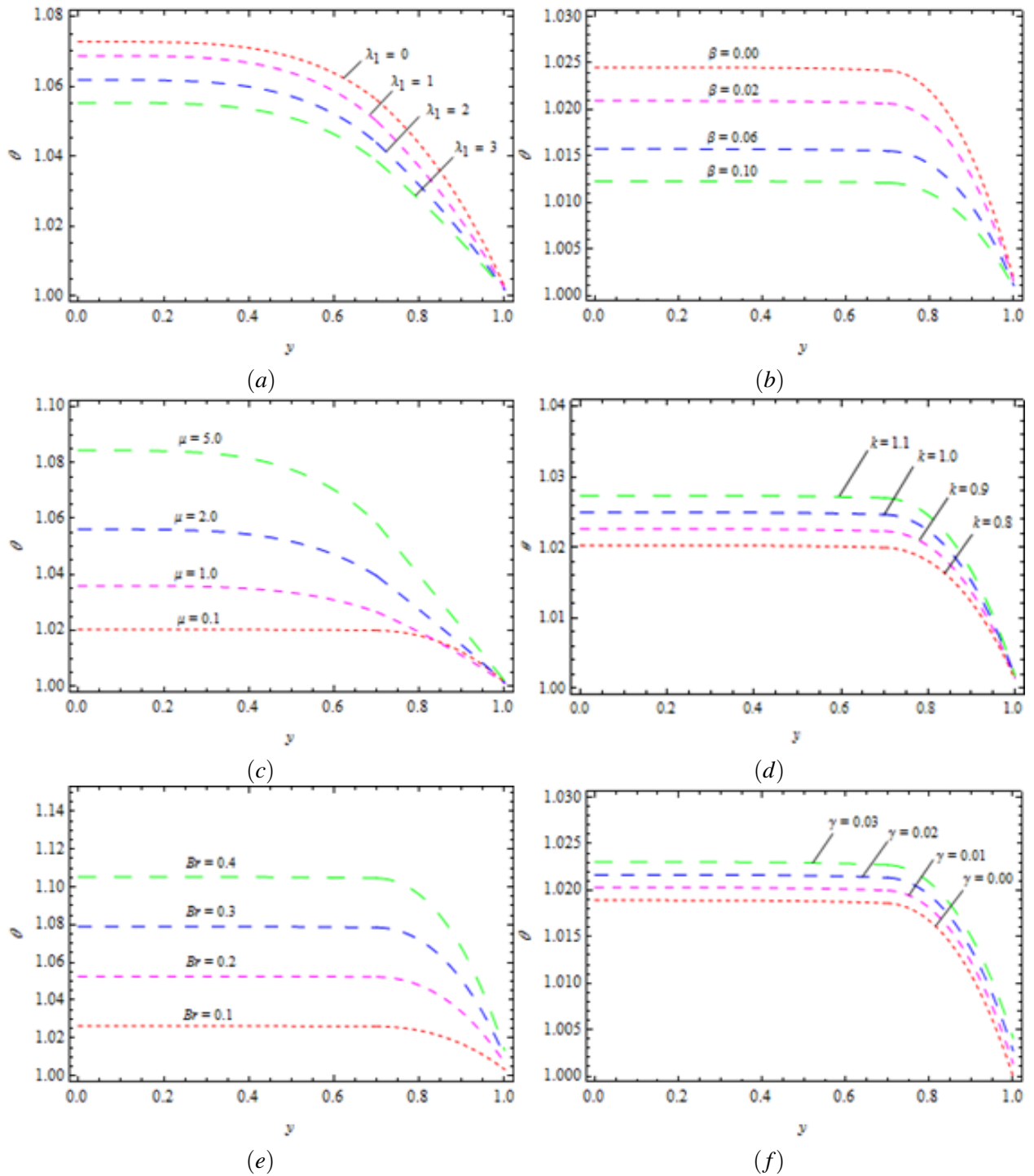


**Fig. 6** Temperature profiles at  $x = 0.5$ ,  $\phi = 0.6$ ,  $\alpha = 0.7$  and  $\bar{Q} = 0.7$  for (a)  $\mu = 1$ ,  $Br = 0.2$ ,  $k = 0.9$ ,  $\beta = 0.01$ ,  $\gamma = 0.01$ ,  $\lambda_1 = 0, 1, 2, 3$ , (b)  $\lambda_1 = 1$ ,  $\mu = 0.1$ ,  $Br = 0.1$ ,  $k = 0.9$ ,  $\gamma = 0.01$ ,  $\beta = 0.00, 0.02, 0.06, 0.10$ , (c)  $\lambda_1 = 1$ ,  $Br = 0.1$ ,  $k = 0.8$ ,  $\beta = 0.01$ ,  $\gamma = 0.01$ ,  $\mu = 0.1, 1.0, 2.0, 5.0$ , (d)  $\lambda_1 = 1$ ,  $Br = 0.1$ ,  $\mu = 0.1$ ,  $\beta = 0.01$ ,  $\gamma = 0.01$ ,  $k = 0.8, 0.9, 1.0, 1.1$  (e)  $\lambda_1 = 1$ ,  $\mu = 0.1$ ,  $k = 1$ ,  $\beta = 0.02$ ,  $\gamma = 0.02$ ,  $Br = 0.1, 0.2, 0.3, 0.4$  (f)  $\lambda_1 = 1$ ,  $\mu = 0.1$ ,  $k = 0.8$ ,  $\beta = 0.1$ ,  $Br = 0.1$ ,  $\gamma = 0.01, 0.02, 0.03, 0.04$ .

### 5 Results and discussion

The shape of interface obtained from Eq. (4.1) is a stream line in the wave frame. The unique interface  $h_1$  is solved from Eq. (4.1) for each in the interval  $(0, h)$  with the help of Mathematica. The effects of the Jef

parameter  $\lambda_1$ , viscosity ratio  $\mu$  and the slip parameter on  $\beta$  the shape of interface are plotted in Fig.2. From Fig. 2(a), we notice that the variation in shape of interface for large Jeffrey parameter gives rise to a thinner peripheral layer in the dilated region. In Fig. 2(b), we found that as the viscosity ratio increases the thickness of the peripheral layer decreases in the dilated region. From Fig. 2(c), we observe that the variation of the interface shape for high slip parameter is associated with thinner peripheral layer in the constricted region. The uniform sinusoidal shape is not seen for the interface.

Equation (3.6) gives the expression for the pressure rise  $\Delta P$  in terms of time averaged flux  $\bar{Q}$ . The effects of  $\lambda_1$ ,  $\mu$  and  $\beta$  on the variation of  $\Delta P$  with  $\bar{Q}$  are computed by numerical quadrature formulae and shown graphically in Fig 3. From Fig. 3(a), it is seen that for large value of viscosity ratio ( $\mu = 10$ ), the pumping rate decreases with increasing  $\lambda_1$  for any appropriately chosen  $\Delta P > 0.8$  and the pumping curves coincides at  $\Delta P = 0.8$ . Further,  $\Delta P < 0.8$ , for the pumping rate increase with an increase in the Jeffrey parameter. Fig. 3(b) indicates that the pumping rate increases with increasing  $\mu$  for any appropriately chosen  $\Delta P > -0.2$ , the pumping curves coincides at  $\Delta P = -0.2$  and below to this value the behavior is opposite. Fig. 3(c) illustrates that for appropriately chosen  $\Delta P > -0.02$ , the pressure rise decreases with increasing  $\beta$  and the trend reversed below to the value of  $\Delta P = -0.02$ .

Equation (3.8) represents the maximum pressure difference  $\Delta P_0$ . Fig.4 is plotted to analyze the effects of  $\lambda_1$ ,  $\beta$  and  $\mu$  on  $\Delta P_0$  with amplitude ratio  $\phi$ . From Figs. 4(a) and 4(b), we found that for a given amplitude ratio, an increase in  $\lambda_1$  and  $\beta$  results in the decrease of  $\Delta P_0$ . Fig.4(c) depicts that for a fixed amplitude ratio,  $\Delta P_0$  increases with increasing  $\mu$ . Further in the limit of  $\phi \rightarrow 0$ , the peristaltic pump approaches to a pressure driven channel flow and in the limit of  $\phi \rightarrow 1$ ,  $\Delta P_0$  becomes indefinitely large. Equation (3.9) gives the expression for the frictional force at the wall  $F$  in terms of time averaged flux  $\bar{Q}$ . The effect of Jeffrey parameter on the frictional force is presented in Fig. 5 and from the figure we infer that the frictional force has opposite behavior compared to pressure rise  $\Delta P$ .

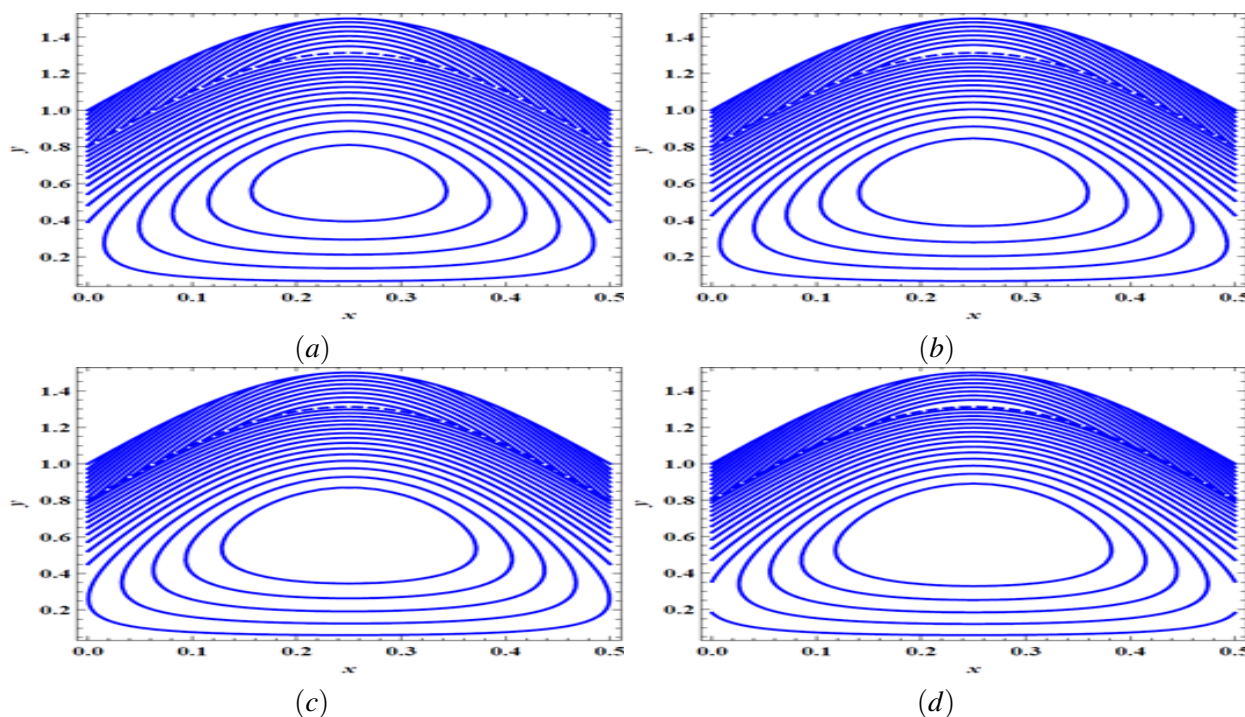


**Fig. 7** Streamlines for (a)  $\lambda_1 = 0.0$  (b)  $\lambda_1 = 0.1$  (c)  $\lambda_1 = 0.2$  (d)  $\lambda_1 = 0.3$  with  $\alpha = 0.8$ ,  $\phi = 0.5$ ,  $\bar{Q} = 0.7$ ,  $\beta = 0.02$ ,  $\mu = 1.2$ .

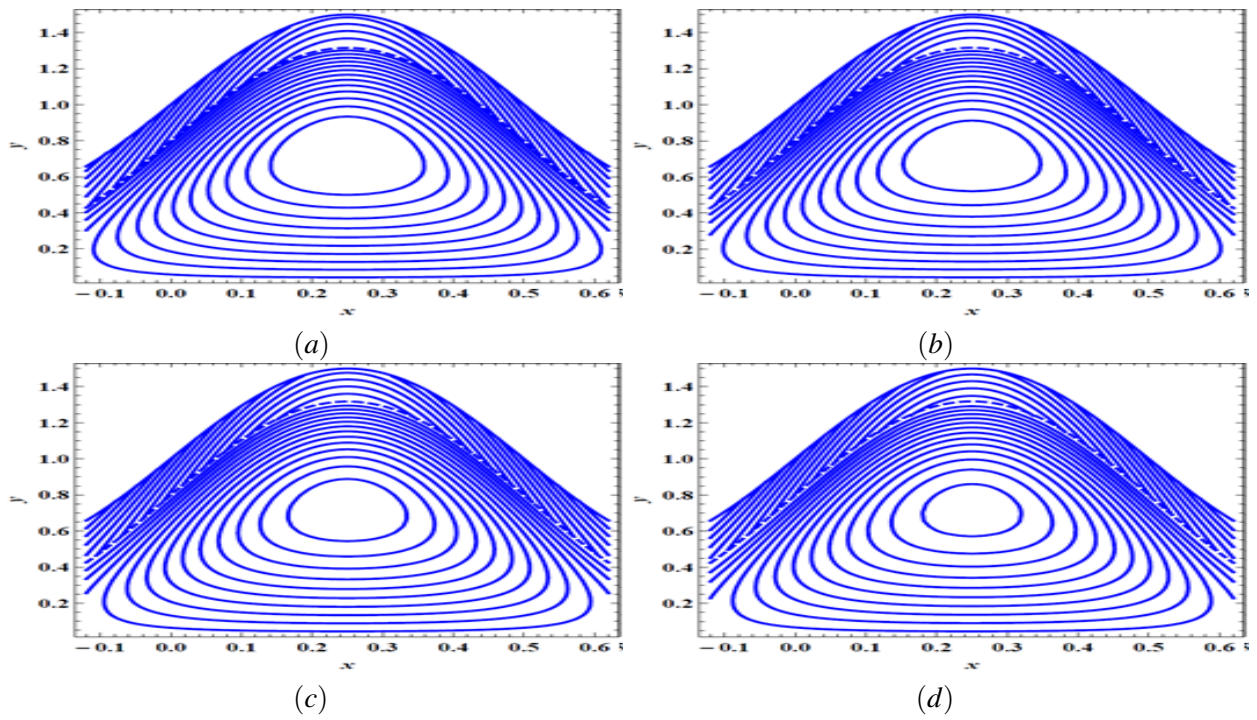


**Fig. 8** Streamlines for (a)  $\beta = 0.00$  (b)  $\beta = 0.01$  (c)  $\beta = 0.02$  (d)  $\beta = 0.03$  with  $\alpha = 0.8$ ,  $\phi = 0.5$ ,  $\bar{Q} = 0.8$ ,  $\lambda_1 = 0.1$ ,  $\mu = 1.2$ .

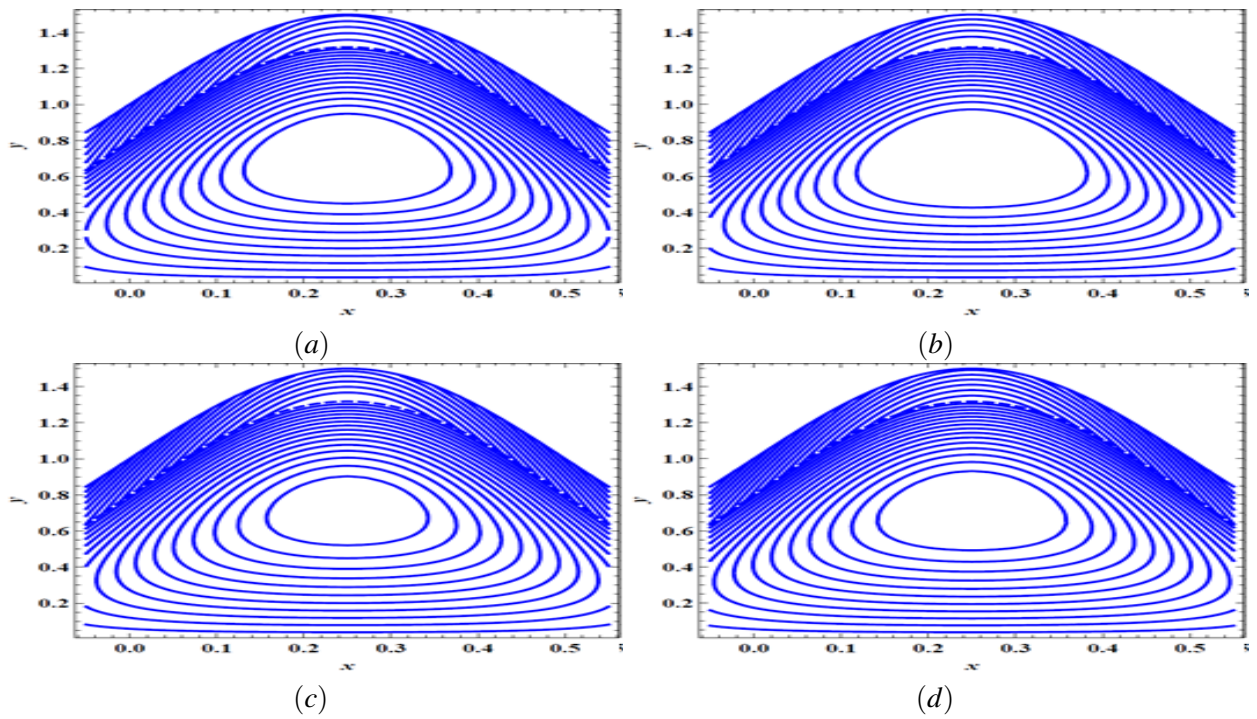


**Fig. 9** Streamlines for (a)  $\mu = 0.09$  (b)  $\mu = 1.0$  (c)  $\mu = 1.1$  (d)  $\mu = 1.2$  with  $\alpha = 0.8$ ,  $\phi = 0.5$ ,  $\bar{Q} = 0.8$ ,  $\lambda_1 = 0.1$ ,  $\beta = 0.02$ .

Temperature field in core and peripheral layers are calculated from Eqs.(3.3) and(3.4) in terms of  $y$ . Temperature profiles are plotted in Figs.6. at an axial station  $x = 0.5$ ,  $\phi = 0.6$  and  $\bar{Q} = 0.7$  to study the effects of  $\lambda_1$ ,  $\beta$ ,  $\mu$ , ratio of thermal conductivity  $k$ , Brinkman number  $Br$  and thermal slip parameter  $\gamma$ , the average thickness of the peripheral layer  $\alpha$ . Fig. 6 (a) and Fig. 6(b) represent the influence of  $\lambda_1$  and  $\beta$  on the variation of temperature distribution  $\theta$ . We find that the temperature decreases with increasing  $\lambda_1$  and  $\beta$  Fig. 6(c) and 6(d) display the temperature behavior with the ratio of viscosity and ratio of thermal conductivity. It is observed that an increase in  $\mu$  and  $k$  results in the increase of  $\theta$ . Fig. 6(e) depicts that the temperature field decreases with an increase in  $Br$ . It is evident from Fig. 6(f) that the temperature increases with increasing  $\gamma$ . Also, we observe that the curves of temperature field are not intersecting at  $\theta = 1$  in presence of thermal slip parameter.

The wave frame stream lines for core and peripheral regions are determined from Eqs. (3.1) and (3.2). Figs. 7-9 are drawn to observe the influences of  $\lambda_1$ ,  $\beta$  and  $\mu$  on the stream line patterns. The shape of interface in the stream line patterns is marked by the dashed line. From Fig.7, we notice that the size of the trapping region increases with an increase in the Jeffrey number. From Fig. 8, we see that the trapping bolus shrinks with an increase in the slip parameter. Fig. 9 shows that the volume of the trapping bolus increases with an increase in the viscosity ratio parameter.

## 6 Conclusions

The present article is concerned with the analysis of peristalsis and heat transfer on the physiological flow of two-fluid model occupying the core region with a Jeffrey fluid and the peripheral region with a Newtonian fluid in a symmetric channel bounded by permeable walls. Analytical solutions for the stream function and the temperature field, interface, pressure rise, frictional force at the wall are determined. The obtained numerical results are presented through graphs and are discussed in detail. We have highlighted here some of the interesting observations.

1. The shape of interface for higher values of Jeffrey parameter  $\lambda_1$  leads to a thinner peripheral layer in the dilated region.
2. In the pumping region ( $\Delta P > 0$ ), the pressure rise decreases with increasing slip parameter  $\beta$ .
3. For a given amplitude ratio, an increase in Jeffrey parameter  $\lambda_1$  and slip parameter  $\beta$  results in a decrease of maximum pressure difference  $\Delta P_0$ .
4. Temperature field decreases by increasing  $\lambda_1$  and  $\beta$  whereas the temperature field increases by increasing thermal slip parameter.
5. An increase in the ratio of viscosity  $\mu$  and ratio of thermal conductivity  $k$  results in the increase of temperature field.
6. The results of no slip conditions can be deduced from this analysis when  $\beta = 0$  and  $\gamma = 0$ .
7. The size of the trapped bolus increases with an increase in the non-Newtonian Jeffrey number and decreases with an increase in the slip parameter.
8. It is observed that when  $\lambda_1 \rightarrow 0$  and  $\beta \rightarrow 0$ , our results agree with those of Brasseur et al.[1] for peristaltic transport of two immiscible Newtonian fluids.

## References

- [1] J. G. Brasseur, S. Corrsin, Nan Q. Lu, The influence of a peripheral layer of different viscosity on peristaltic pumping with Newtonian fluids, *J. Fluid Mech.* 174(1987) 495 -519.

- [2] J. G. Brasseur, A fluid mechanical perspective on esophageal bolus transport, *Dysphagia* 2 (1987) 32-39.
- [3] G. Bugliarello, J. Sevilla, Velocity distribution and other characteristics of steady and pulsatile blood flow in fine glass tubes, *Biorheology* 7(2) (1970) 85-107.
- [4] G. R. Cokelet, The rheology of human blood: In Biomechanics, its foundation and objectives, (Prentice-Hall, Englewood Cliffs, New Jersey, 1972), pp. 63-103.
- [5] U. Farooq, T. Hayat, A. Alsaedi, Shijun Liao, Heat and mass transfer of two-layer flows of third-grade nano-fluids in a vertical channel, *Appl. Math. Comput.* 242 (2014) 528 -540.
- [6] D. J. Griffiths, Dynamics of the upper urinary tract: I. Peristaltic flow through a distensible tube of limited length, *Phys. Med. Biol.* 32(7) (1987) 813 -822.
- [7] Tasawar Hayat, Nasir Ali, Peristaltic motion of a Jeffrey fluid under the effect of a magnetic field in a tube, *Commun. Nonlinear Sci. Numer. Simul* 13 (2008) 1343 - 1352.
- [8] T. Hayat, S. Hina, Effects of heat and mass transfer on peristaltic flow of Williamson fluid in a non-uniform channel with slip conditions, *Int. J. Numer. Meth. Fluids* (2010) DOI: 10.1002/flid.2433.
- [9] A. Kavitha, R. H. Reddy, A.N.S. Srinivas, S. Sreenadh, R. Saravana, Peristaltic pumping of a Jeffrey fluid between porous walls with suction and injection, *International Journal of Mechanical and Materials Engineering (IJMME)* 7(2) (2012) 152-157.
- [10] A. Kavitha, R. Hemadri Reddy, R. Saravana, S. Sreenadh, Peristaltic transport of a Jeffrey fluid in contact with a Newtonian fluid in an inclined channel, *Ain Shams Engineering Journal* (2015) <http://dx.doi.org/10.1016/j.asej.2015.10.014>.
- [11] M. Kothandapani, S. Srinivas, Peristaltic transport of a Jeffrey fluid under the effect of magnetic field in an asymmetric channel, *Int. J. Nonlinear Mech.* 43 (2008) 915 - 924.
- [12] Masako Sugihara-Sekia, Bingmei M. Fu, Blood flow and permeability in microvessels, *Fluid Dyn. Res.* 37 (2005) 82-132.
- [13] Kh. S. Mekheimer, Peristaltic flows of blood under effect of a magnetic field in a non-uniform channels, *Appl. Math. Comput.* 153 (2004) 763-777.
- [14] J.C. Misra, S.K. Pandey, [A Mathematical Model for Oesophageal Swallowing of a Food Bolus](#), *Math. Comput. Modell.* 33 (2001) 997-1009.
- [15] J. C. Misra, S. K. Pandey, [Peristaltic transport of blood in small vessels: study of a mathematical model](#), *Comput. Math. Appl.* 43 (2002) 1183 - 1193.
- [16] S. Nadeem, Safia Akram, Slip effects on the peristaltic flow of a Jeffrey fluid in an asymmetric channel under the effect of induced magnetic field, *Int. J. Numer. Meth. Fluids* 63 (2010) 374 -394.
- [17] Noreen Sher Akbar, S. Nadeem, and Mohamed Ali, Jeffrey fluid model for blood flow through a tapered artery with a stenosis, *J. Mech. Med. Biol.* 11 (2011) 529-545.
- [18] Noreen Sher Akbar, T. Hayat, S. Nadeem, Awatif A. Hendi, Effects of slip and heat transfer on the peristaltic flow of a third order fluid in an inclined asymmetric channel, *Int. J. Heat Mass Transfer* 54 (2011) 1654-1664.
- [19] Noreen Sher Akbar and S. Nadeem, [Simulation of Variable Viscosity and Jeffrey Fluid Model for Blood Flow Through a Tapered Artery with a Stenosis](#), *Commun. Theor. Phys.* 57(1) (2012) 133-140.
- [20] Noreen Sher Akbar, S. Nadeem, Changhoon Lee, Characteristics of Jeffrey fluid model for peristaltic flow of chyme in small intestine with magnetic field, *Results in Physics* 3 (2013) 152-160.
- [21] S. K. Pandey, D. Tripathi, Unsteady model of transportation of Jeffrey fluid by peristalsis, *Int. J. Biomath* 3(4) (2010) 473-491.
- [22] R. Ponalagusamy, R. Tamil Selvi, Influence of magnetic field and heat transfer on two-phase fluid model for oscillatory blood flow in an arterial stenosis, *Meccanica* 50 (2015) 927-943.
- [23] A. Ramachandra Rao, S. Usha, Peristaltic transport of two immiscible viscous fluids in a circular tube, *J. Fluid Mech.* 298 (1995) 271-285.
- [24] G. Ravikumur, G. Radhakrishnamacharya, Effect of homogeneous and heterogeneous chemical reactions on peristaltic transport of a Jeffrey fluid through a porous medium with slip condition, *J. Appl. Fluid Mech.* 8(3) (2015) 521- 528.
- [25] P. G. Saffman, On the Boundary Conditions at the Surface of a Porous Medium, *Stud. Appl. Math.* 1 (1971) 93-101.
- [26] A.H. Shapiro, M.Y. Jaffrin, S.L. Weinberg, Peristaltic pumping with long wavelengths at low Reynolds number, *J. Fluid Mech.* 37 (1969) 799-825.
- [27] L. M. Srivastava, V. P. Srivastava, Peristaltic transport of a two-layered model of physiological fluid, *J. Biomech.* 15 (1982) 257-265.
- [28] L. M. Srivastava, V. P. Srivastava, Peristaltic transport of blood, Casson model-II, *J. Biomech.* 17(1984) 821-829.
- [29] L.M. Srivastava, V. P. Srivastava, Peristaltic transport of a power-law fluid: applications to the ductus efferentes of the reproductive tract, *Rheol. Acta* 27 (1988) 428-433.
- [30] Dharmendra Tripathi, A mathematical model for the peristaltic flow of chyme movement in small intestine, *Math. Biosci.* 233 (2011) 90-97.
- [31] J. C. Umavathi, I. C. Liu, M. Shekar Unsteady mixed convective heat transfer of two immiscible fluids confined between long vertical wavy wall and parallel flat wall, *Appl. Math. Mech.* -Engl Ed 33(7) (2012) 931-950.

- [32] S. Usha, A. Ramachandra Rao, Peristaltic transport of two layered Power-law fluids, *Trans. ASME, J. Biomech. Engng.* 119(1997) 483-488.
- [33] K. Vajravelu, S. Sreenadh, V. Ramesh Babu, Peristaltic pumping of a Herschel-Bulkley fluid in contact with a Newtonian fluid, *Q. Appl. Math.* 64(4) (2006) 593 -604.
- [34] K. Vajravelu, S. Sreenadh, R. Hemadri Reddy, K. Murugesan, Peristaltic Transport of a Casson fluid in contact with a Newtonian Fluid in a Circular Tube with permeable wall, *Int. J. Fluid Mech. Res.* 36(3)(2009) 244-254.
- [35] K. Vajravelu, S. Sreenadh, R. Saravana, Combined influence of velocity slip, temperature and concentration jump conditions on MHD peristaltic transport of a Carreau fluid in a non-uniform channel, *Appl. Math. Comput.* 225(2013) 656-676.
- [36] K. Vajravelu, S. Sreenadh, P. Lakshminarayana G. Sucharitha, The effect of heat transfer on the nonlinear peristaltic transport of a Jeffrey fluid through a finite vertical porous channel, *Int. J. Biomath.* 7(2) (2016) 1650023, 1-24.

©UP4 Sciences. All rights reserved.